JOURNAL OF CHEMICAL & ENGINEERING DATA

ARTICLE

pubs.acs.org/jced

Carbon Dioxide Adsorption Isotherms on Activated Carbons

Bidyut Baran Saha,*[,†] Skander Jribi,[‡] Shigeru Koyama,[‡] and Ibrahim I. El-Sharkawy[§]

[†]Department of Mechanical Engineering, Faculty of Engineering, Kyushu University, 744, Motooka, Nishi-ku, Fukuoka-shi 819-0395, Japan

[‡]Department of Energy and Environmental Engineering, Interdisciplinary Graduate School of Engineering Sciences, Kyushu University, 6-1 Kasuga-koen, Kasuga-shi, Fukuoka 816-8580, Japan

[§]Mechanical Power Engineering Department, Faculty of Engineering, Mansoura University, El-Mansoura, Egypt

ABSTRACT: This paper presents adsorption isotherm data of CO_2 onto two different types of highly porous activated carbons (ACs) for temperatures ranging from (−18 to 80) °C and pressures up to 10 MPa. The assorted adsorbents are activated carbon fiber (ACF) of type A-20 and activated carbon powder of type Maxsorb III. Adsorption isotherm data have been obtained using a volumetric technique and fitted to the Dubinin−Astakhov (D−A), Tóth, Langmuir, and modified D−A equations. The latter considers the pseudosaturation pressure of CO_2 that plays an important role for supercritical gas adsorption, and the pseudosaturation pressure was determined from the experimental data. The Tóth and modified D−A isotherms correlate with the experimental data within 5 % root-mean-square deviation (rmsd) and present a better fitting than that of the Langmuir and the D−A equations. The isosteric heat of adsorption data were derived from the Tóth and modified D−A isotherm equations and the correlation proposed by Chakraborty et al., and the average heat of adsorption values were found to be comparable. These data are essential for designing CO_2-based adsorption cooling, refrigeration, and gas storage systems.

INTRODUCTION

Physical adsorption on carbonaceous adsorbents has been extensively studied for the separation and purification of gases,[1−3] gas storage,[4−6] and adsorption cooling[7−11] applications. For the adsorption cooling and adsorbed gas storage applications, it is essential to estimate correct isotherms and isosteric heat of adsorption of the assorted adsorbent−adsorbate pairs for designing adsorption systems. Using these key data, the numerical modeling of the processes of chiller operation and gas storage performance can be performed with a high level of confidence.

As one of the countermeasures against global warming and energy conservation problems, Saha et al.[8] and El-Sharkawy et al.[12] investigated experimentally the adsorption characteristics of ethanol and methanol, respectively, onto activated carbon fiber and Maxsorb III. However, these adsorbent−refrigerant pairs work on subatmospheric pressures, and thus the system footprint becomes large. Accordingly, it is inevitable to develop adsorption cooling systems based on natural working pairs which work above atmospheric pressure. Among natural refrigerants, CO_2 has the advantage of having no problems related to flammability and toxicity as opposed to ammonia and thus has received considerable attention especially in the field of automotive air conditioners.

Himeno et al.[13] reported a systematic study of the adsorption of carbon dioxide onto five different activated carbons using the static volumetric method. Experiments were performed at temperatures ranging from (0 to 50) °C and pressures up to 6 MPa. However, CO_2-based transcritical adsorption cooling systems can go up to 10 MPa. From the above perspective, the adsorption isotherms of CO_2 on two different types of highly porous activated carbons for temperatures ranging from (−18 to 80) °C and pressures up to 10 MPa were determined as these data are not available in the open literature. Experimental data were correlated with the D−A, modified D−A, Tóth, and Langmuir isotherm models. The isosteric heat of adsorption data are also evaluated.

EXPERIMENTAL SECTION

Materials. The adsorbents used in this study are ACF of type A-20 and activated carbon powder of type Maxsorb III, and these activated carbons were developed by AD'ALL Co. Ltd., Japan, and Kansai Coke & Chemicals Co. Ltd., Japan, respectively. The microporus ACF (A-20) has a large surface area of 2000 $m^2 \cdot g^{-1}$, micropore volume (v_μ) of 1.03 $cm^3 \cdot g^{-1}$, and average pore diameter of 21.6 Å.[7] It is suitable for physical adsorption and easy to pack. On the other hand, Maxsorb III has a surface area as high as 3150 $m^2 \cdot g^{-1}$, micropore volume of 1.7 $cm^3 \cdot g^{-1}$, and mean pore diameter of 2 nm.[14] Samples of CO_2 and helium were supplied by Asahi Sanso Shokai Ltd. Japan having a purity of 99.995 %.

Experimental Apparatus. Measurements of the adsorption equilibrium of CO_2 onto Maxsorb III and ACF (A-20) have been conducted using a volumetric technique. Figure 1 shows the schematic diagram of the experimental apparatus which comprises: (i) adsorption and load cells, and these cells are designed to stand a pressure of 12 MPa; (ii) two water baths of type Advantec TBN402DA connected with two water circulators of type Eyela CTP-3000 and CTP-6000; and (iii) a 25.8 μm mesh is attached at the center of the adsorption cell. The adsorption cell

Received: September 27, 2010
Accepted: February 25, 2011
Published: March 15, 2011

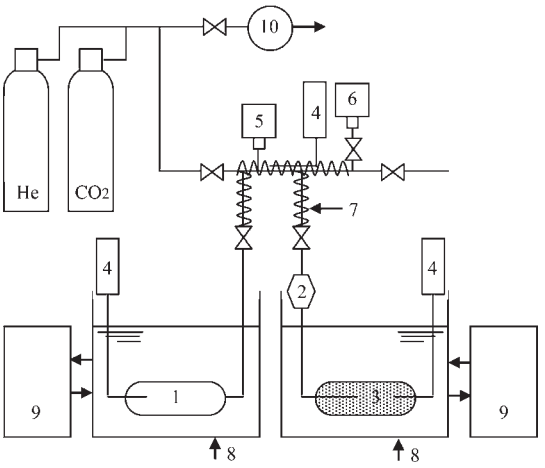

Figure 1. Schematic diagram of volumetric experimental apparatus (1, load cell; 2, filter; 3, adsorption cell; 4, thermocouple; 5, pressure transducer; 6, vacuum gauge; 7, tape heater; 8, water bath; 9, water circulator; 10, vacuum pump).

is connected to the load cell through 1/4" stainless steel plumbing and a set of Swagelok fittings (connectors, T's, and reducers). Other parts are stopping valves of type SS-1KS4, safety valves of type SS-4R3A, and 15 μm pore size filter of type SS-4TF-15. The tubes shown by zigzag lines in Figure 1 are mounted by a tape heater to control their temperatures.

Instrumentation. The instrumentation used in the present study was: (i) a vacuum pressure gauge of type Phil PG-D5A, (ii) a 10 MPa absolute pressure transducer of type Kyowa PHS-100KA with an uncertainty of ± 0.2 % of full scale in measurement, (iii) several K type thermocouples within ± 0.1 °C uncertainty calibrated with a standard platinum resistance thermometer, and (iv) a data acquisition system comprising a Yokogawa MX data logger and a personal computer to record the experimental data each second.

Procedure. Before conducting experiments, the volume of load and adsorption cells along with their connecting tubes are measured using a water filling method by measuring the mass of pure water filled in the cell using a digital balance of type Mettler Toledo PR8002 with ± 0.01 g uncertainty. At first, the assorted adsorbent was dried in an electric oven at a temperature of 373 K for 12 h and then packed in the adsorption cell. The mass of the dried adsorbent packed in the adsorption cell was also measured prior to the adsorption isotherm experiment. Adsorption isotherm measurements were performed according to the following chronological steps:

(i) Both of the load and adsorption cells are evacuated with a vacuum pump for 6 h until the pressure reaches as low as 20 Pa. At the same time, the activated carbon packed inside the adsorption cell is being regenerated with a band heater, and the temperature is maintained at 120 °C.

(ii) A certain amount of CO_2 is released into the loading cell where the equilibrium is reached within 30 min. The state of the gas in terms of pressure and temperature is then recorded using the data acquisition system.

(iii) The valve between the adsorption cell and the load cell is opened. The starting of adsorption is characterized by a sharp increase of the adsorption bed temperature and a pressure drop from the loading pressure to near the equilibrium pressure, which are shown in Figure 2. The adsorption cell reaches its equilibrium in about an hour, and then the equilibrium pressure is recorded. Then, steps (ii) and (iii) are repeated until reaching the saturation pressure at the assorted adsorption isotherm temperature or the maximum pressure of the CO_2 cylinder which is typically about 6 MPa.

(iv) To measure the adsorption equilibrium for pressures above 6 MPa, the load cell is used as an intermediate vessel to increase the pressure. At first, the load cell is connected to the CO_2 cylinder and cooled to increase the mass of adsorbate in the cell. After that, the load cell is isolated from the CO_2 cylinder and heated until the load pressure increases to the desired value.

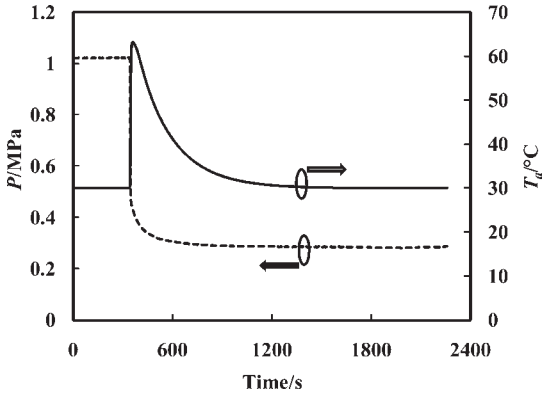

Figure 2. Evolution of pressure and temperature during adsorption.

Assuming that adsorption occurs in micropores, the void volume, V_{void}, is calculated by the following equation.

$$V_{void} = V_{cell} - \frac{m_{ch}}{\rho_s} - v_\mu m_{ch} \quad (1)$$

where the third term in the RHS of eq 1 is the void volume correction. V_{cell} stands for the volume of adsorption cell; m_{ch}, ρ_s, and v_μ denote the mass, solid density, and micropore volume of the activated carbon, respectively.

A mass of 16.82 g of ACF (A-20) has been packed into the adsorption cell of 76.38 cm^3, assuming a solid density of carbon (ρ_s) of 1.8 $g \cdot cm^{-3}$ as stated by the ACF manufacturer, and the adsorption cell void is 67.03 cm^3. This value is in good agreement with the cell void measured by helium expansion. Taking into account the micropore volume (v_μ), the void volume (V_{void}) in the adsorption cell packed with ACF (A-20) is found to be 48.53 cm^3.

With the same approach, a mass of 18.67 g of Maxsorb III is packed into a second cell of 80.27 cm^3, with $\rho_s/g \cdot cm^{-3} = 2.2$ for Maxsorb III, and the adsorption cell void is 71.78 cm^3. V_{void} in this case is estimated to be 40.04 cm^3.

Data Reduction. The primary data are the load pressure P_l, the equilibrium pressure P_{eq}, the load temperature T_l, and the adsorbent temperature T_a. The mass adsorbed in the n^{th} measurement can be determined by eq 2 below, where n varies from 1 to 7.

$$m_n = m_{n-1} + \Delta m_{load,n} - \Delta m_{void,n} \quad (2)$$

where m_{n-1} is the previous amount adsorbed; $\Delta m_{load,n}$ is the mass difference in the load cell between the load state and equilibrium state; and $\Delta m_{void,n}$ is the mass added to the void volume.

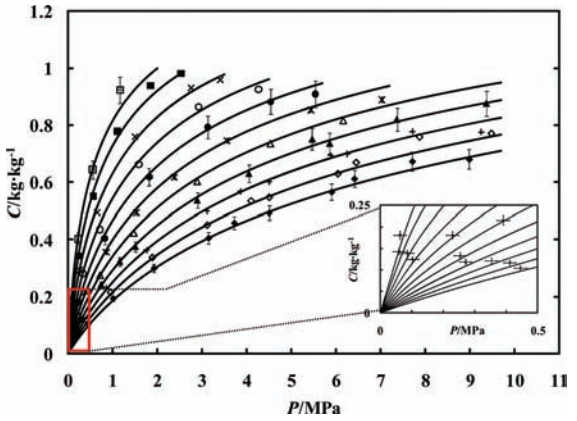

Figure 3. Adsorption isotherm of CO_2 on ACF (A-20) with ± 5 % error bars in uptake and ± 0.02 MPa horizontal error bars in pressure: □, −18.8 °C; ■, −10 °C; ×, 0 °C; ○, 10 °C; ●, 20 °C; ∗, 30 °C; Δ, 40 °C; ▲, 50 °C; +, 60 °C; ◇, 70 °C; ♦, 80 °C; solid lines are from the Tóth model.

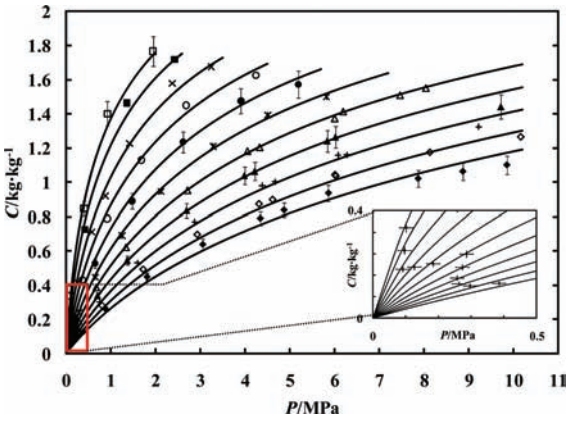

Figure 4. Adsorption isotherm of CO_2 on Maxsorb III with ± 5 % error bars in uptake and ± 0.02 MPa horizontal error bars in pressure: □, −17.6 °C; ■, −10 °C; ×, 0 °C; ○, 10 °C; ●, 20 °C; ∗, 30 °C; Δ, 40 °C; ▲, 50 °C; +, 60 °C; ◇, 70 °C; ♦, 80 °C; solid lines are from the Tóth model.

The experiments measure excess adsorption, and correlations relate absolute adsorption. The adsorbed phase volume is assumed to be negligible compared to the bulk gas phase volume.

Correlation of Isotherms. Adsorption experimental data were correlated with four different isotherms, namely, Langmuir, Tóth, Dubinin−Astakhov (D−A), and modified D−A equations.

Langmuir and Tóth Isotherms. The well-known Langmuir and Tóth isotherm models can be expressed by eqs 3 and 4, respectively.[15]

$$\frac{C}{C_0} = \frac{bP}{1+bP} \tag{3}$$

$$\frac{C}{C_0} = \frac{bP}{(1+(bP)^t)^{1/t}} \tag{4}$$

where $C/\mathrm{kg\cdot kg^{-1}}$ is the amount adsorbed; $C_0/\mathrm{kg\cdot kg^{-1}}$ is the saturated amount adsorbed; P/MPa is the equilibrium pressure; and $b/\mathrm{MPa^{-1}}$ is the adsorption affinity given by

$$b = b_0 e^{(Q/RT)} \tag{5}$$

where b_0 is the adsorption affinity at infinite temperature and Q is the isosteric heat of adsorption. The parameter t in eq 4 is said to characterize the system heterogeneity which is a characteristic of the adsorbent or adsorbate or a combination of both. The lower the value of t, the more heterogeneous the system. If t is equal to unity, the Tóth isotherm is reduced to the Langmuir isotherm.

D−A Isotherm. The Dubinin−Astakhov (D−A) model is given by[16]

$$W = W_0 \exp\left[-\left(\frac{A}{E}\right)^n\right] \tag{6}$$

where $W/\mathrm{cm^3\cdot g^{-1}}$ is the volume adsorbed; $W_0/\mathrm{cm^3\cdot g^{-1}}$ is the limiting micropore volume; $E/\mathrm{J\cdot mol^{-1}}$ is the characteristic energy; n is the structural heterogeneity parameter; and A is the adsorption potential. The adsorbed phase volume $W/\mathrm{cm^3\cdot g^{-1}}$ is obtained by multiplying the adsorption uptake $C/\mathrm{kg\cdot kg^{-1}}$ by the molar volume V_m which can be expressed as[17]

$$V_m = V_t \exp(\alpha(T - T_t)) \tag{7}$$

where V_t is the molar volume of the liquid adsorbate at the triple point (T_t = 216.6 K and P_t = 0.51814 MPa) and the numerical value of V_t is found to be 0.84858 $\mathrm{cm^3\cdot g^{-1}}$. The thermal expansion of the superheated liquid α is taken as 0.0025 $\mathrm{K^{-1}}$ as suggested by Ozawa.[17] It is noteworthy to mention here that the values of V_m which are found by the present method are almost identical to those of Cook and Basmadjian.[18] The adsorption potential A is given by

$$A = RT \ln\left(\frac{P_s}{P}\right) \tag{8}$$

where R is the gas constant; P_s is the saturated vapor pressure at the temperature T; and P is the equilibrium pressure. At high pressure, the pressure should be replaced by the fugacity to correct for the nonideality of gases. The adsorption potential becomes

$$A = RT \ln\left(\frac{f_s}{f}\right) \tag{9}$$

where f and f_s are the corresponding fugacities of P and P_s, respectively.

Above the critical temperature (T_c) of CO_2, the concept of liquid is nonexistent. Dubinin suggested the following empirical equation to compute the values of the pseudovapor pressure above the critical temperature.[19]

$$P_s = \left(\frac{T}{T_c}\right)^2 P_c \text{ for } (T > T_c) \tag{10}$$

Modified D−A Model. Amankwah and Schwarz[20] proposed a modified D−A model where the estimation of pseudovapor pressures takes into account the interactions between the adsorbate−adsorbent system and is given by

$$P_s = \left(\frac{T}{T_c}\right)^k P_c \tag{11}$$

Table 1. Raw Adsorption Data of CO_2 onto ACF (A-20) for Adsorption Temperatures of (−10, 10, 30, 50, and 70) °C

measurement number	T_l/°C	P_l/MPa	T_a/°C	P_{eq}/MPa	Δm_{load}/g	Δm_{void}/g	m_n/g	C/kg·kg^{-1}
1	30	0.491	−10	0.060	2.463	0.061	2.402	0.143
2	30	0.843	−10	0.239	3.549	0.182	5.768	0.343
3	30	1.208	−10	0.572	3.870	0.355	9.283	0.553
4	30	1.795	−10	1.108	4.464	0.617	13.130	0.782
5	30	2.382	−10	1.853	3.735	0.989	15.876	0.947
6	30	2.778	−10	2.535	1.854	1.115	16.615	0.992
1	30	0.486	10	0.103	2.196	0.096	2.101	0.125
2	30	0.824	10	0.339	2.858	0.226	4.733	0.282
3	30	1.199	10	0.713	2.982	0.371	7.344	0.438
4	30	2.281	10	1.585	4.801	0.945	11.200	0.668
5	30	3.556	10	2.931	5.231	1.785	14.646	0.876
6	30	4.617	10	4.266	3.757	2.614	15.789	0.947
1	30	1.056	30	0.391	3.980	0.346	3.634	0.217
2	30	1.311	30	0.860	2.807	0.433	6.008	0.358
3	30	1.982	30	1.536	3.003	0.664	8.347	0.498
4	30	2.784	30	2.382	3.029	0.911	10.465	0.625
5	30	3.965	30	3.565	3.691	1.482	12.674	0.759
6	30	5.770	30	5.438	5.160	3.241	14.593	0.878
7	32	7.201	30	7.037	7.316	6.499	15.411	0.935
1	50	0.683	50	0.272	2.229	0.224	2.005	0.120
2	50	1.184	50	0.745	2.476	0.401	4.080	0.243
3	50	1.999	50	1.512	2.953	0.684	6.349	0.379
4	50	3.485	50	2.897	4.126	1.367	9.108	0.545
5	50	4.420	50	4.053	2.927	1.309	10.726	0.643
6	50	6.275	50	5.866	4.385	2.518	12.594	0.758
1	32	1.925	50	1.159	4.985	1.235	3.750	0.326[a]
2	32	6.171	50	5.472	11.194	6.126	8.818	0.771[a]
3	39	7.564	50	7.367	5.192	4.311	9.699	0.852[a]
4	45	9.531	50	9.373	8.858	8.053	10.504	0.931[a]
1	30	0.799	70	0.412	2.290	0.320	1.970	0.118
2	30	1.292	70	0.955	2.105	0.435	3.641	0.218
3	30	2.299	70	1.890	2.873	0.788	5.726	0.343
4	30	3.484	70	3.121	3.064	1.122	7.668	0.460
5	30	4.781	70	4.508	3.068	1.408	9.328	0.560
6	30	6.206	70	6.047	3.240	1.793	10.775	0.649
1	35	5.146	70	4.102	10.805	4.550	6.254	0.546[a]
2	35	6.710	70	6.458	5.058	3.437	7.875	0.690[a]
3	35	7.906	70	7.877	3.631	2.549	8.957	0.787[a]
4	36	9.708	70	9.488	3.749	3.538	9.168	0.809[a]

[a] The mass of ACF (A-20) is taken as 11.56 g.

where k is a constant obtained from the fitting of experimental adsorption isotherm data. This modified D−A equation provides better fitting in the case of the adsorption isotherm of methane and hydrogen onto four types of activated carbons.[20] The k values vary from 2.1 to 2.73 for methane and from 2.72 to 4.16 for hydrogen. For CO_2 adsorption on ACF (A-20) and Maxsorb III, k is found to be 3.86 and 4.49, respectively.

Isosteric Heat of Adsorption. Knowledge of the thermodynamic properties of the adsorbent + adsorbate system allows better understanding of the adsorption process. The determination of heat of adsorption permits measurement of the degree of energetic heterogeneity of gas−solid interactions. The Clausius−Clapeyron (CC) equation has been widely used to estimate the heat of adsorption (ΔH) from isotherm equations and can be expressed as

$$\Delta H_{CC} = RT^2 \left(\frac{\partial \ln P}{\partial T}\right)_C \quad (12)$$

The ΔH_{CC} derived from the Langmuir and Tóth isotherms is constant and is equal to the parameter Q in eq 5. The ΔH_{CC} derived from the modified D−A equation reduces to

$$\Delta H_{CC,D-A} = RT^2 \frac{\partial \ln P_s}{\partial T} + A + \frac{\alpha}{n} TE^n A^{1-n} \quad (13)$$

where $RT^2(\partial \ln P_s)/(\partial T) = kRT$ for $T > T_c$.

Recently, from the rigor of thermodynamic formalisms, Chakraborty et al.[21] modified the Clausius−Clapeyron heat of

Table 2. Raw Adsorption Data of CO_2 onto Maxsorb III for Adsorption Temperatures of (−10, 10, 30, 50, and 70) °C

measurement number	T_l/°C	P_l/MPa	T_a/°C	P_{eq}/MPa	Δm_{load}/g	Δm_{void}/g	m_n/g	C/kg·kg^{-1}
1	27	0.906	−10	0.097	4.801	0.078	4.722	0.253
2	27	1.848	−10	0.423	9.086	0.274	13.534	0.725
3	27	3.311	−10	1.355	14.672	0.876	27.329	1.464
4	27	3.180	−10	2.425	6.047	1.285	32.091	1.719
1	30	0.754	10	0.127	3.652	0.096	3.556	0.190
2	30	1.139	10	0.363	4.669	0.182	8.044	0.431
3	30	2.014	10	0.918	7.147	0.450	14.741	0.790
4	30	2.670	10	1.683	7.033	0.684	21.090	1.130
5	30	3.543	10	2.687	7.031	1.052	27.069	1.450
6	30	4.769	10	4.249	5.670	2.364	30.375	1.627
1	27	1.059	30	0.286	4.665	0.203	4.462	0.239
2	27	1.315	30	0.653	4.138	0.269	8.332	0.446
3	27	1.994	30	1.252	5.006	0.461	12.877	0.690
4	27	2.843	30	2.121	5.493	0.728	17.641	0.945
5	27	3.939	30	3.290	6.044	1.132	22.554	1.208
6	27	4.905	30	4.509	4.897	1.454	25.996	1.392
7	27	6.016	30	5.824	4.223	2.220	27.999	1.500
1	30	0.763	50	0.257	2.963	0.170	2.793	0.150
2	30	1.325	50	0.705	3.836	0.305	6.324	0.339
3	30	2.015	50	1.368	4.333	0.473	10.184	0.545
4	30	3.485	50	2.697	6.449	1.039	15.594	0.835
5	30	4.473	50	3.989	4.940	1.159	19.375	1.038
6	30	6.333	50	6.025	6.519	2.301	23.593	1.264
1	32	6.031	50	4.218	23.220	3.379	19.841	1.063
2	32	6.136	50	5.840	5.156	1.836	23.160	1.241
3	45	9.962	50	9.724	12.627	8.876	26.911	1.441
1	27	0.708	70	0.297	2.440	0.185	2.255	0.121
2	27	1.330	70	0.811	3.276	0.329	5.202	0.279
3	27	2.368	70	1.727	4.586	0.615	9.173	0.491
4	27	3.481	70	2.935	4.691	0.876	12.988	0.696
5	27	4.697	70	4.316	4.402	1.111	16.279	0.872
6	27	6.203	70	6.013	4.756	1.575	19.461	1.042
1	32	6.093	70	4.620	20.130	3.378	16.752	0.897
2	32	6.246	70	6.034	3.894	1.334	19.312	1.034
3	32	8.351	70	8.133	5.025	2.415	21.921	1.174
4	42	10.332	70	10.164	4.775	3.088	23.609	1.265

adsorption equation (eq 12) by introducing an extra term (second term of the RHS of eq 14), which accounts for the heat of adsorbed mass with respect to pressure and temperature changes during adsorption, and the modified equation is expressed by

$$\Delta H_{ads} = RT^2 \left(\frac{\partial \ln P}{\partial T}\right)_C + Tv_g \left(\frac{\partial P}{\partial T}\right) \quad (14)$$

Accordingly, the corrected heat of adsorption employing the modified D−A equation reduces to

$$\Delta H_{ads,D-A} = kRT + A + \frac{\alpha}{n} TE^n A^{1-n} + Tv_g \left(\frac{\partial P}{\partial T}\right) \quad (15)$$

RESULTS AND DISCUSSION

The experimental uptake curves of CO_2 onto ACF (A-20) and Maxsorb III for temperatures ranging from (−18 to 80) °C and pressures up to 10 MPa are shown in Figures 3 and 4, respectively. The shape of the adsorption isotherms of CO_2 in the assorted microporous materials is monotonically concave and therefore can be classified as type I in the IUPAC classification.[22] The raw data for CO_2 adsorption on ACF (A-20) and Maxsorb III are presented in Table 1 and Table 2, respectively.

The experimental data are fitted with the Langmuir, Tóth, Dubinin−Astakhov (D−A), and modified D−A isotherm equations. A nonlinear optimization routine is used to optimize the parameters of these models to fit the experimental data for multiple temperatures.[15] The root-mean-square deviation (rmsd) between the calculated values (cal) and experimental data (exp) is defined as

$$\text{rmsd} = \sqrt{\frac{\sum_0^N \left(\frac{C_{exp} - C_{cal}}{C_{exp}} \cdot 100\right)^2}{N}} \quad (16)$$

As can be seen from Figures 3 and 4, the maximum uptake of CO_2 onto ACF (A-20) near the saturation pressure is 1 kg of

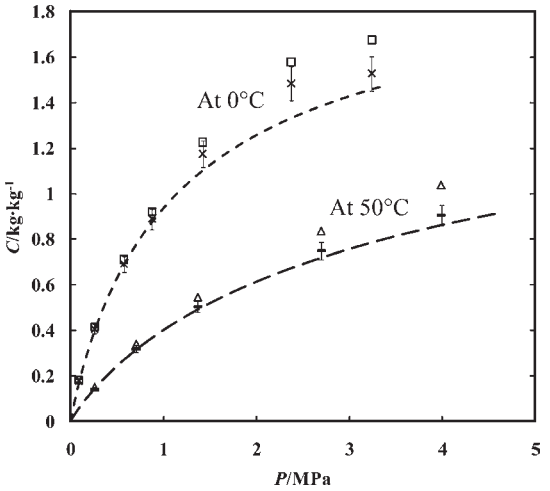

Figure 5. Comparison of adsorption isotherm data of CO_2 on Maxsorb III: ×, present study with ± 5 % error bars and without void volume correction; □, present study with void volume correction; −, present study with ± 5 % error bars and without void volume correction; Δ, present study with void volume correction; broken lines, Himeno et al.[13]

Table 3. Fitting Parameters of Langmuir and Tóth Models for CO_2 Adsorption onto ACF (A-20) and Maxsorb III

adsorbent	model	C_0/kg·kg^{-1}	b_0/MPa^{-1}	Q/kJ·mol^{-1}	t	rmsd
A-20	Langmuir	1.22	$2.21 \cdot 10^{-4}$	19.41	-	8.24
	Tóth	1.56	$2.55 \cdot 10^{-4}$	19.23	0.696	3.40
Maxsorb III	Langmuir	2.21	$1.06 \cdot 10^{-4}$	20.56	-	7.85
	Tóth	3.06	$1.17 \cdot 10^{-4}$	20.37	0.664	3.77

CO_2 per kg of ACF (A-20), and that of CO_2 onto Maxsorb III is 1.7 kg of CO_2 per kg of Maxsorb III. In both cases, each experimental point is found within ± 5 % deviation with the Tóth model.

A comparison of adsorption isotherm data for pressure up to 4.5 MPa between CO_2 adsorption onto Maxsorb III and those of the Himeno[13] data for a similar adsorbent is shown in Figure 5. For isotherm temperatures of (0 and 50) °C, the present adsorption isotherm data without void volume correction are similar to those of Himeno's data. The data with void volume corrections are higher by about (5 to 10) % compared to those without void volume corrections.

The fitting parameters of the Langmuir and Tóth equations for the adsorption of CO_2 onto ACF (A-20) and Maxsorb III are presented in Table 3. The Langmuir equation presents a higher rmsd between the experimental adsorption data and the fitting model. The rmsd for the Langmuir model is found to be 8.24 % and 7.85 % for CO_2 adsorption on ACF (A-20) and Maxsorb III, respectively. The Tóth model correlates the experimental uptake with lower rmsd than the Langmuir model as it considers the heterogeneity effect of the adsorbent−adsorbate pairs (parameter t which is below 0.7). The rmsd values for the Tóth isotherm are found to be 3.4 % and 3.77 % for ACF (A-20) and Maxsorb III, respectively.

The plots of adsorbed volume W versus the adsorption potential A, where A is calculated from eqs 9 and 10, are presented in Figure 6(a) for the adsorption of CO_2 onto ACF (A-20). These plots are supposed to follow one single line independent of temperature, known as the characteristic curve

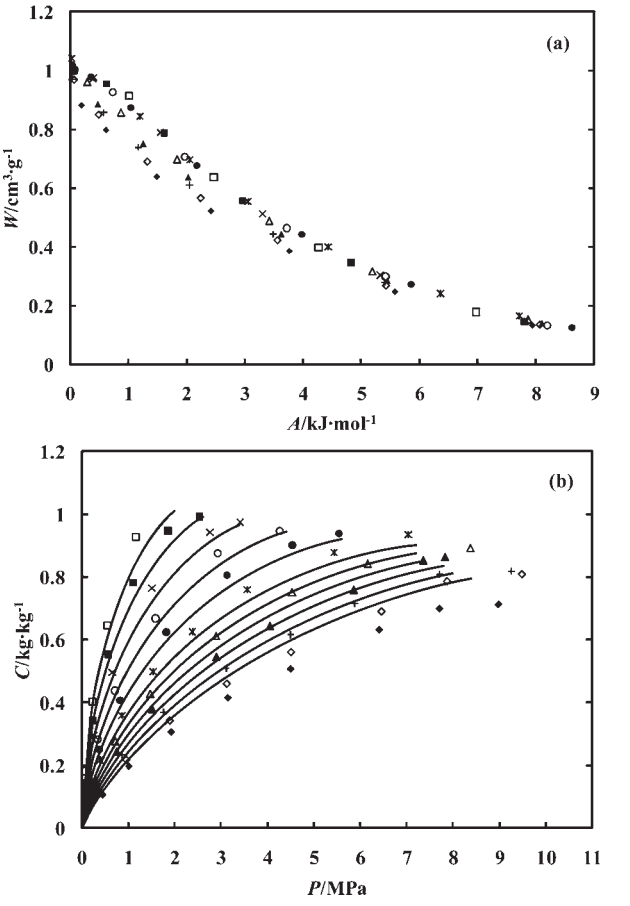

Figure 6. (a) Characteristic curve for the ACF (A-20)−CO_2 pair and (b) adsorption isotherms of CO_2 onto ACF (A-20) using the D−A equation for k = 2: □, −18.8 °C; ■, −10 °C; ×, 0 °C; ○, 10 °C; ●, 20 °C; ∗, 30 °C; Δ, 40 °C; ▲, 50 °C; +, 60 °C; ◇, 70 °C; ♦, 80 °C.

which is an index of goodness of the fit of the D−A model. As can be seen from Figure 6(a), a scatter is observed in the characteristic curve, and accordingly, deviations between experimental adsorption isotherm data and the D−A model are observed in Figure 6(b). These deviations are due to the low-estimated pseudo vapor pressures P_s which are related to the adsorbate only and do not take into account the nature of the adsorbent.[20] To overcome this problem, an additional parameter k is added to the D−A model. This constant is used to estimate the corrected pseudo vapor pressure values and is obtained directly from the fit of experimental adsorption data to the modified D−A model.

The effect of the parameter k on the characteristic curve and the adsorption isotherms of CO_2 onto ACF (A-20) is shown in Figures 7(a) and 7(b), respectively. An improved single characteristic curve for all isotherm temperatures is obtained. Moreover, the error between the experimental adsorption uptake and the modified D−A model becomes less than ± 5 %. The same trends are found for the characteristic curves and adsorption isotherms of CO_2 onto Maxsorb III, and these are not presented in this paper.

The fitting parameters of the D−A and modified D−A equations for the adsorption of CO_2 onto ACF (A-20) and Maxsorb III are presented in Table 4. The D−A equation yields higher rmsd's as high as 6.61 % for ACF (A-20) and 9.58 % for Maxsorb III. However, the use of the modified D−A equation

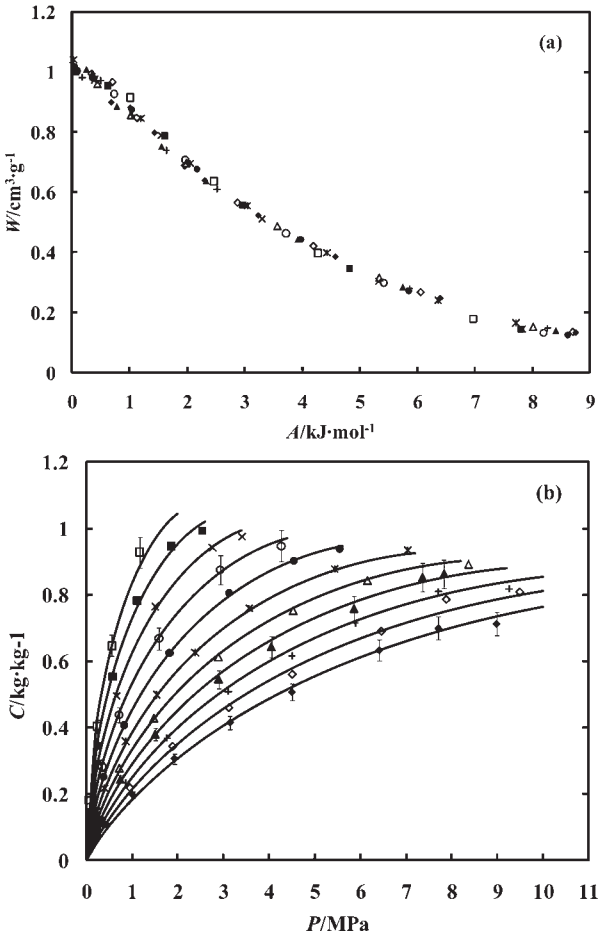

Figure 7. (a) Characteristic curve for the ACF (A-20)−CO_2 pair and (b) adsorption isotherms of CO_2 onto ACF (A-20) using the modified D−A equation for k = 3.86: □, −18.8 °C; ■, −10 °C; ×, 0 °C; ○, 10 °C; ●, 20 °C; ∗, 30 °C; Δ, 40 °C; ▲, 50 °C; +, 60 °C; ◇, 70 °C; ♦, 80 °C.

Table 4. Fitting Parameters of D−A and Modified D−A Models for CO_2 Adsorption onto ACF (A-20) and Maxsorb III

adsorbent	model	k	W_0/cm³·g^{-1}	E/J·mol^{-1}	n	rmsd
A-20	D−A	2	1.002	4468.22	1.14	6.61
	modified D−A	3.86	1.03	4549.92	1.18	3.58
Maxsorb III	D−A	2	1.727	3983.24	1.12	9.58
	modified D−A	4.49	1.759	4159.89	1.18	4.53

reduces the rmsd as low as 3.58 % and 4.53 % for ACF (A-20) and Maxsorb III, respectively.

The plots of the heat of adsorption versus the adsorbed amount for ACF (A-20)−CO_2 and Maxsorb III−CO_2 pairs are shown in Figures 8(a) and 8(b), respectively. The Clausius−Clapeyron heats of adsorption (ΔH_{CC}) derived from the Tóth isotherm equation are constant, and these are equal to (19.23 and 20.37) kJ·mol^{-1} for ACF (A-20)−CO_2 and Maxsorb III−CO_2 pairs, respectively. On the other hand, the isosteric heat of adsorption (ΔH_{ads}) proposed by Chakraborty et al.[21] yields higher isosteric heat of adsorption values than those obtained from $\Delta H_{CC,D-A}$. It is noteworthy to mention that for both adsorbent−adsorbate pairs the values of $\Delta H_{ads,D-A}$ are higher than those obtained from the Tóth equation during low loading

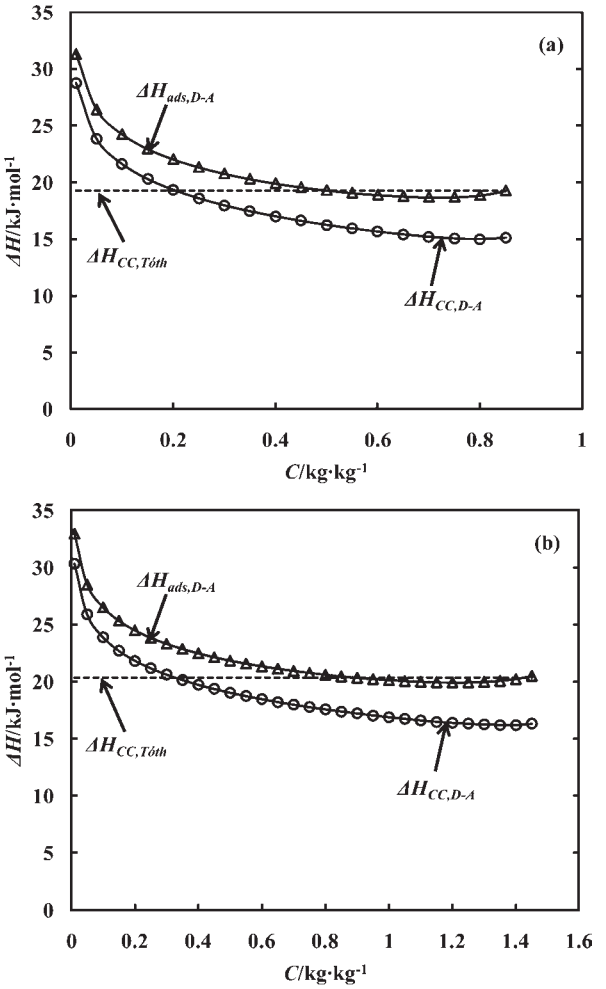

Figure 8. (a) Heat of adsorption for the ACF (A-20)−CO_2 pair and (b) heat of adsorption for the Maxsorb III−CO_2 pair: ---, ΔH_{CC} derived from the Tóth isotherm; ○, ΔH_{CC} derived from the modified D−A equation (eq 13); Δ, corrected heat of adsorption derived from the modified D−A equation (eq 15).

and are almost the same during relatively higher loading where C is above 0.5 kg·kg^{-1} for ACF (A-20) and above 0.8 kg·kg^{-1} for Maxsorb III.

■ CONCLUSIONS

Adsorption isotherm data for CO_2 onto ACF (A-20) and Maxsorb III have been obtained through a volumetric technique. The adsorption uptake measurements cover the temperature ranging from (−18 to 80) °C and pressures up to 10 MPa. The data have been successfully correlated to popular isotherm equations within ± 5 % uncertainty. For the measured adsorption isotherm data, an improvement in accuracy has been observed in the present study over that of an earlier method for the similar adsorbent−adsorbate pairs. Adsorption uptake of CO_2 on Maxsorb III is about 1.7 times higher than that of ACF (A-20). The isosteric heat of adsorption data have been extracted from the experimental measurements, which appear to be well interpreted from that derived from the modified D−A equation. The average heats of adsorption of CO_2 in Maxsorb III and ACF (A-20) are found to be (20.37 and 19.23) kJ·mol^{-1}, respectively.

dx.doi.org/10.1021/je100973t |J. Chem. Eng. Data 2011, 56, 1974–1981

AUTHOR INFORMATION

Corresponding Author

*Phone: +81-92-802-3101. Fax: +81-92-802-3125. E-mail: saha@mech.kyushu-u.ac.jp.

ACKNOWLEDGMENT

The authors wish to express their thanks to their former colleague, Dr. Kuwahara, for his help during the experimental work.

REFERENCES

(1) Majlan, E. H.; Daud, W. R. W.; Iyuke, S. E.; Mohamad, A. B.; Kadhum, A. A. H.; Mohammad, A. W.; Takriff, M. S.; Bahaman, N. Hydrogen purification using compact pressure swing adsorption system for fuel cell. *Int. J. Hydrogen Energy* **2009**, *34*, 2771–2777.

(2) Yates, M.; Blanco, J.; Avila, P.; Martin, M. P. Honeycomb monoliths of activated carbons for effluent gas purification. *Microporous Mesoporous Mater.* **2000**, *37*, 201–208.

(3) Knoblauch, K. Activated carbon and carbon molecular sieves in gas separation and purification. *Gas Sep. Purif.* **1993**, *7*, 195–196.

(4) Saha, B. B.; Koyama, S.; El-Sharkawy, I. I.; Habib, K.; Srinivasan, K.; Dutta, P. Evaluation of adsorption parameters and heats of adsorption through desorption measurements. *J. Chem. Eng. Data* **2007**, *52*, 2419–2424.

(5) Himeno, S.; Komatsu, T.; Fujita, S. Development of a new effective biogas adsorption storage technology. *Adsorption* **2005**, *11* (1 SUPPL.), 899–904.

(6) Sircar, S.; Golden, T. C.; Rao, M. B. Activated carbon for gas separation and storage. *Carbon* **1996**, *34*, 1–12.

(7) El-Sharkawy, I. I.; Kuwahara, K.; Saha, B. B.; Koyama, S.; Ng, K. C. Experimental investigation of activated carbon fibers/ethanol pairs for adsorption cooling system application. *Appl. Thermal Eng.* **2006**, *26*, 859–865.

(8) Saha, B. B.; El-Sharkawy, I. I.; Chakraborty, A.; Koyama, S. Study on an activated carbon fiber-ethanol adsorption chiller: Part II — performance evaluation. *Int. J. Refrig.* **2007**, *30*, 96–102.

(9) Saha, B. B.; Chakraborty, A.; Koyama, S.; Ng, K. C.; Sai, M. A. Performance modelling of an electro-adsorption chiller. *Philos. Mag.* **2006**, *86*, 3613–3632.

(10) Al Mers, A.; Azzabakh, A.; Mimet, A.; El Kalkha, H. Optimal design study of cylindrical finned reactor for solar adsorption cooling machine working with activated carbon−ammonia pair. *Appl. Thermal Eng.* **2006**, *26*, 1866–1875.

(11) Critoph, R. E.; Metcalf, S. J.; Tamainot-Telto, Z. Proof of concept car adsorption air-conditioning system using a compact sorption reactor. *Heat Transfer Eng.* **2010**, *31*, 950–956.

(12) El-Sharkawy, I. I.; Hassan, M.; Saha, B. B.; Koyama, S.; Nasr, M. M. Study on adsorption of methanol onto carbon based adsorbents. *Int. J. Refrig.* **2009**, *32*, 1579–1586.

(13) Himeno, S.; Komatsu, T.; Fujita, S. High-pressure adsorption equilibria of methane and carbon dioxide on several activated carbons. *J. Chem. Eng. Data* **2005**, *50*, 369–376.

(14) Saha, B. B.; Chakraborty, A.; Koyama, S.; Yoon, S.; Mochida, L.; Kumja, M.; Yap, C.; Ng, K. C. Isotherms and thermodynamics for the adsorption of n-butane on pitch based activated carbon. *Int. J. Heat Mass Transfer* **2008**, *51*, 1582–1589.

(15) Do, D. D. Adsorption Analysis: Equilibria and Kinetics. *Series in Chem. Eng.*; Imperial College Press: 1998.

(16) Dubinin, M. M. Fundamentals of the theory of adsorption in micropores of carbon adsorbents: Characteristics of their adsorption properties and microporous structures. *Carbon* **1989**, *27*, 457–467.

(17) Ozawa, S.; Kusumi, S.; Ogino, Y. Physical adsorption of gases at high pressure. IV. An improvement of the Dubinin-Astakhov adsorption equation. *J. Colloid Interface Sci.* **1976**, *56*, 83–91.

(18) Agarwal, R. K.; Schwarz, J. A. Analysis of high pressure adsorption of gases on activated carbon by potential theory. *Carbon* **1988**, *26*, 873–887.

(19) Dubinin, M. M. *Prog. Surface and Membrane Science*; Cadenhead, D. A., Eds. et al. ; Academic Press: New York, 1975; Vol. 9, Ch. 1.

(20) Amankwah, K. A. G.; Schwarz, J. A. A. Modified approach for estimating pseudo-vapor pressures in the application of the Dubinin-Astakhov equation. *Carbon* **1995**, *33*, 1313–1319.

(21) Chakraborty, A.; Saha, B. B.; Koyama, S.; Ng, K. C. On the thermodynamic modeling of the isosteric heat of adsorption and comparison with experiments. *Appl. Phys. Lett.* **2006**, *89*, 171901.

(22) Sing, K. S. W.; Everett, D. H.; Haul, R. A. W.; Moscoul, L.; Pierotti, R. A.; Rouqerol, J.; Siemieniewska, T. Reporting Physisorption Data for Gas/Solid Systems with Special Reference to the Determination of Surface Area and Porosity. *Pure Appl. Chem.* **1985**, *57*, 603–619.